Sinusoidal Hydraulic Testing of a Multi-Layer Aquifer at the Waste Isolation Pilot Plant, Carlsbad, NM, USA

Todd C. Rasmussen*, Nathanial J. Toll†, and Mark Bakker‡
The University of Georgia, Athens 30602

February 15, 2013

Abstract. The Waste Isolation Pilot Plant, located near Carlsbad, New Mexico, USA, is an operating repository for transuranic nuclear materials. Performance testing and monitoring is routinely conducted at the site to ensure that the facility is operating as designed. Three sinusoidal aquifer tests were performed by pumping at a periodic rate in the Culebra Dolomite Member of the Rustler Formation, a hydrogeologic unit that overlies the repository and a hypothetical pathway for repository releases. Drawdowns in nearby observation wells displayed sinusoidal behavior, with drawdown amplitudes that diminished – and time lags that increased – with distance from the pumping well. An analytic solution was developed to obtain the hydraulic properties of the two dominant units (Lower and Upper) within the vertically heterogeneous Culebra Dolomite using the sinusoidal data. The problem is approached mathematically using a matrix formulation that vertically discretizes the section into multiple layers and employs eigenvalues and eigenvectors to evaluate a Bessel function with complex matrix arguments. The solution for pumping from discrete intervals within an isotropic aquifer is consistent with a partially penetrating solution. While the multi-layer approach confirms previous hydraulic properties in the more conductive Lower Culebra, new information about spatial variability in the less conductive Upper Culebra is provided.

Keywords. Hydrogeology; sinusoidal aquifer tests; multi-layer aquifer; Culebra Dolomite; Waste Isolation Pilot Plant

*Corresponding author, *trasmuss@uga.edu*
†Rio Tinto, Australia
‡Delft Technical University, The Netherlands

1 Introduction

Demonstrating the integrity of waste isolation in geologic media requires the adequate characterization of pathways and transport rates. Hydrogeologic properties needed to provide this information are conventionally found using hydraulic testing that involves the extraction of water at constant or stepwise-variable rates, which may produce large volumes of water that require costly disposal or treatment. Another concern during aquifer tests is the effect of background interference (e.g., precipitation, streamflow, barometric pressure, earth tides) that introduce uncertainty in the estimation of hydrogeologic properties. While the rate or duration of water extraction can be increased to minimize the interference caused by background sources, the resulting dewatering or depressurization of the formation may alter formation properties, affect boundary conditions, and perhaps alter local and regional flow gradients.

Sinusoidal pumping provides an alternative method for performing aquifer tests (Black and Kipp, 1981; Streltsova, 1988; Bruggeman, 1999; Rasmussen et al., 2003; Bakker, 2004). A sinusoidal drawdown response in the aquifer is created by adjusting the withdrawal rate so that the drawdown in the pumping well oscillates with a prescribed period and amplitude. Wells near the pumping borehole are used to determine the drawdown amplitude attenuation and phase lag (time delay) of the signal between the pumping and observation wells. Aquifer properties more accurately represent ambient conditions because the magnitude of the hydraulic disturbance is reduced.

01 Tanmoy Das

Analytic solutions for sinusoidal drawdowns in observation wells are available for confined aquifers (Black and Kipp, 1981; Bruggeman, 1999), partially penetrating wells (Haborak, 1999; Rasmussen et al., 2003), leaky aquifers (Haborak, 1999; Rasmussen et al., 2003; Tang and Jiao, 2001), one-dimensional aquifers (Carr and van der Kamp, 1969; Townley, 1995), two-dimensional aquifers (Sun, [illegible]), composite aquifers (Trefry, 1999), and near cylindrical inhomogeneities (Bakker, 2009).

02 Tanmoy Das

While these solutions are appropriate in many single-layer applications, their use where multiple layers of differing permeability are present could result in important hydraulic properties being ignored. Analytic solutions are available for multilayer aquifers, but only for steady or step-wise constant pumping (Bruggeman, 1966, 1999; Neuman and Witherspoon, 1969a,b; Javandel and Witherspoon, 1983; Hemker and Maas, 1987; Maas, 1987; Hemker, 1999). Analytic solutions for sinusoidal pumping in multilayer aquifers have not been published, to the authors' knowledge.

A new solution extends previous sinusoidal solutions to conditions where vertical variation within the aquifer is present, both due to vertical variation in aquifer hydraulic properties, as well as pumping from different levels within a vertically homogeneous aquifer. The multi-layer solution consists of multiple horizontal layers with either equivalent or vertically varying hydraulic properties. Applications using multiple equivalent properties include the need to interpret conditions when pumping is limited

to partial penetration, or to conditions when multiple, non-adjacent intervals are pumped.

The new multi-layer analytic solution is used to estimate aquifer hydraulic properties from drawdowns measured in seven wells during three sinusoidal aquifer tests within two intervals of the Culebra Dolomite Member, which is part of the Rustler Formation at the Waste Isolation Pilot Plant (WIPP) site, a repository for transuranic wastes located in southeastern New Mexico, USA.

2 Approach

Consider an aquifer where drawdown, $s(r,t)$, varies periodically over time, t, as a function of distance, r, from a pumping well. The governing partial differential equation for this problem is:

$$D\,\nabla^2 s = \frac{\partial s}{\partial t} \tag{1}$$

where D is the aquifer hydraulic diffusivity, with $D = T/S$ for a confined aquifer with transmissivity T and storativity S, or $D = K/S_s$ for general flow with hydraulic conductivity K and specific storage S_s.

We are only concerned with the drawdown response to periodic pumping at a specified frequency, and assume that all other non-periodic, quasi-periodic, and other periodic functions (i.e., those not at the pumping frequency) do not affect the drawdown at the pumping frequency, or are removed from the data prior to analysis (Townley, 1995; Bruggeman, 1999; Rasmussen et al., 2003; Bakker, 2004). This assumption leads to the boundary conditions:

$$s(r = \infty, \forall t) = 0 \tag{2}$$

$$Q(r = 0, \forall t) = Q_1 \cos \omega t - Q_2 \sin \omega t = \mathcal{A}_Q \exp \imath(\omega t + \mathcal{P}_Q) \tag{3}$$

where Q is the periodic pumping rate, $\omega = 2\pi/p$ is the pumping frequency with period p, $\mathcal{A}_Q = \sqrt{Q_1^2 + Q_2^2}$ and $\mathcal{P}_Q = \arctan(Q_2/Q_1)$ are the pumping rate amplitude and phase, respectively, and $\imath = \sqrt{-1}$ is the imaginary unit.

The resulting periodic drawdown is:

$$s(\forall r, \forall t) = \mathcal{A}_s \exp \imath(\omega t + \mathcal{P}_s) \tag{4}$$

where $\mathcal{A}_s$ and $\mathcal{P}_s$ are the drawdown amplitude and phase, respectively.

Fig 1 illustrates the behavior of aquifer drawdowns in response to periodic pumping. Note that drawdown lags the pumping rate, the duration of which is the *phase lag*. Note also that drawdown and pumping rate magnitudes can be determined by the *amplitude* of the periodic signal.

We can conceptualize flow through a single aquifer as having both horizontal and vertical flux, q_h and q_v, given by:

$$q_h = -K_h \frac{\partial s}{\partial r} \qquad q_v = -K_v \frac{\partial s}{\partial z} \tag{5}$$

where K_h and K_v are the horizontal and vertical hydraulic conductivities (if different), and z is the vertical dimension. This leads to the formulation:

$$m\, K_h\, \nabla^2 s = \frac{K_v}{m'}\, s + m\, S_s \frac{\partial s}{\partial t} \tag{6}$$

where m is the thickness of each layer, and m' is the vertical distance between the midpoints of each layer.

Eqn 6 assumes that vertical flow is only a function of the drawdown within the aquifer, and that the overlying and/or underlying layers are unaffected by the drawdown. Fig 2 (top) provides a conceptual diagram illustrating flow through a single-layer aquifer.

Substitution of Eqn 4 into Eqn 1, and finding the derivatives gives:

$$\left[K_h\, \nabla^2 s\right]\, e^{\imath\omega t} = \left[\frac{K_v}{m\, m'}\, s\right]\, e^{\imath\omega t} + \left[\imath\omega S_s\, s\right]\, e^{\imath\omega t} \tag{7}$$

Canceling common terms yields:

$$K_h\, \nabla^2 s = \frac{K_v}{m\, m'}\, s + \imath\omega S_s\, s = \left[\frac{K_v}{m\, m'} + \imath\omega S_s\right]\, s \tag{8}$$

yielding:

$$\nabla^2 s = u\, s \tag{9}$$

where

$$u = \frac{1}{K_h}\, \left[\frac{K_v}{m\, m'} + \imath\omega S_s\right] \tag{10}$$

which is the same as:

$$u = \frac{1}{B^2} + \imath\, \frac{\omega}{D} \tag{11}$$

where $B = \sqrt{m\, K_h/(K_v/m')}$, and $D = K/S_s$ is the hydraulic diffusivity.

The solution for Eqn 9 is composed of the Bessel functions (Maas, 1986):

$$s = a\, I_o[r\sqrt{u}] + b\, K_o[r\sqrt{u}] \tag{12}$$

where I_o and K_o are the modified Bessel functions of the first and second kinds, respectively, of zero order. The coefficients, a and b, are found using the boundary conditions:

$$\lim_{r\to\infty} s = 0 \tag{13}$$

$$\lim_{r\to 0}\left[r\frac{\partial s}{\partial r}\right] = \frac{Q}{2\pi T} \tag{14}$$

where $T = m\,K_h$ is the aquifer transmissivity.

The resulting solution through a single aquifer is given by:

$$s = \frac{Q}{2\pi T}\,K_o[r\sqrt{u}] \tag{15}$$

which is consistent with existing confined and leaky solutions (Rasmussen et al., 2003).

Eqn 15 applies to flow in a single layer. Flow through a multi-layer aquifer system can be described using the matrix representation:

$$\mathbf{T}\,\nabla^2\vec{s} = [\mathbf{L} + \imath\omega\mathbf{S}]\;\vec{s} \tag{16}$$

where $\vec{s}$ is a column vector of drawdowns in each layer, s_ℓ, $\mathbf{T}$ and $\mathbf{S}$ are the diagonal matrices of transmissivity and storativity, respectively, whose diagonal elements contain the values for each layer, $\mathrm{diag}[\mathbf{T}] = T_\ell = (m\,K)_\ell$ and $\mathrm{diag}[\mathbf{S}] = S_\ell = (m\,S_s)_\ell$, and whose off-diagonal elements are zeroes, and $\mathbf{L}$ is a tridiagonal matrix that accounts for the vertical components of flow between layers:

$$\mathbf{L} = \begin{bmatrix} L(1,2) & -L(1,2) & 0 & 0 & \cdots \\ -L(1,2) & L(1,2)+L(2,3) & -L(2,3) & 0 & \cdots \\ 0 & -L(2,3) & L(2,3)+L(3,4) & -L(3,4) & \cdots \\ \vdots & & & \ddots & \vdots \\ 0 & 0 & \cdots & -L(n-1,n) & L(n-1,n) \end{bmatrix} \tag{17}$$

where $L = K_v/m'$, with K_v and m' being the interlayer (vertical) hydraulic conductivity and thickness, respectively.

Eqn 17 implies that the multiple aquifer system is bounded above and below by geologic units that do not contribute to flow within the aquifer, and that vertical flow between layers depends on the interlayer hydraulic gradient. Fig 2 (bottom) illustrates the multilayer conceptual model.

Multiplying Eqn 16 by the inverse of the transmissivity matrix yields:

$$\nabla^2\vec{s} = \mathbf{u}\,\vec{s} \tag{18}$$

where:

$$\mathbf{u} = \mathbf{T}^{-1}\,(\mathbf{L} + \imath\omega\mathbf{S}) \tag{19}$$

As previously, the general solution to this matrix ordinary differential equation is:

$$\vec{s} = \mathrm{K}_o\left[r\sqrt{\mathbf{u}}\right]\;\vec{a} + \mathrm{I}_o\left[r\sqrt{\mathbf{u}}\right]\;\vec{b} \tag{20}$$

where K_o and I_o are modified Bessel functions of complex matrix arguments, and $\vec{a}$ and $\vec{b}$ are column vectors with constants to be determined using specified boundary conditions, including $\vec{s} = 0$ as $r \to \infty$, which leads to $\vec{b} = \vec{0}$ because of the behavior of K_o and I_o at infinity, and:

$$\vec{Q} = \lim_{r \to o} \left[-2\pi r \, \mathbf{T} \, \frac{\mathrm{d}\vec{s}}{\mathrm{d}r} \right] \tag{21}$$

Differentiation of Eqn 15 with respect to r gives:

$$\frac{\mathrm{d}\vec{s}}{\mathrm{d}r} = -\sqrt{\mathbf{u}} \; \mathrm{K}_1 \left[r\sqrt{\mathbf{u}} \right] \; \vec{a} \tag{22}$$

Substitution of Eqn 22 into Eqn 21 and knowing that (Abramowitz and Stegun, 1972, Eqn 9.6.9):

$$\lim_{u \to o} u \, \mathrm{K}_1[u] = 1 \tag{23}$$

yields:

$$\vec{a} = -\, \mathbf{T}^{-1} \, \frac{\vec{Q}}{2\pi} \tag{24}$$

Combining these equations provides the solution for $\vec{s}$ in complex matrix form:

$$\vec{s} = \mathrm{K}_o \left[r\sqrt{\mathbf{u}} \right] \; \mathbf{T}^{-1} \, \frac{\vec{\mathrm{Q}}}{2\pi} \tag{25}$$

where the amplitude and phase vectors are $\vec{\mathcal{A}}_s = \mathtt{amp}[\vec{s}]$ and $\vec{\mathcal{P}}_s = \mathtt{arg}[\vec{s}]$, respectively, with components $(\vec{\mathcal{A}}_f)_\ell = \mathtt{amp}[\vec{s}_\ell]$ and $(\vec{\mathcal{P}}_s)_\ell = \mathtt{arg}[\vec{s}_\ell]$.

The final step is to evaluate the modified Bessel function, K_o, for a matrix argument, $\mathbf{u}$, which is accomplished using (Maas, 1986):

$$F[\mathbf{u}] = \mathbf{x} \, F[\mathbf{v}] \, \mathbf{x}^{-1} \tag{26}$$

where $\mathbf{x}$ and $\mathbf{v}$ are the eigenvectors and associated eigenvalues of $\mathbf{u}$, respectively, and noting that a function of a diagonal matrix equals the matrix of the function applied to each diagonal element.

3 Synthetic Experiments

Three synthetic experiments are used to evaluate the analytic approach for interpreting sinusoidal aquifer tests in multilayer media. The first experiment assumes that the aquifer is confined, homogeneous, isotropic, and of infinite extent and uniform thickness. A second experiment assumes the aquifer is anisotropic, with a vertical hydraulic conductivity that is one-tenth the horizontal ($K_v = K_h/10$). The final experiment assumes that the upper half of the aquifer has one-tenth the hydraulic conductivity of the lower half ($K_u = K_l/10$).

For the first experiment, the aquifer is subdivided into ten layers of equal thicknesses (m_ℓ = 1 m, $m = \sum m_\ell$ = 10 m) and hydraulic properties ($D = T/S$ = 1 m^2/s, $T = 10^{-6}$ m^2/s, $S = 10^{-6}$, $L = 10^{-6}$ s^{-1}). Three pumping scenarios were tested; a) from all ten layers (ℓ=1-10), b) from the upper half (ℓ=6-10), and c) from the upper tenth (ℓ=10). The amplitude of the periodic pumping rate and lag in each pumping layer are $\mathcal{A}_Q = 10^{-6}$ m^3/s/m and $\mathcal{P}_Q = 0$ for all pumping scenarios.

Drawdowns obtained from the matrix solutions are compared to the periodic solution for a partially penetrating well in a homogeneous, confined aquifer (Haborak, 1999; Rasmussen et al., 2003):

$$s = \frac{Q}{2\pi T}\left[\mathrm{K}_o[r\sqrt{v}] - \sum_{k=1}^{\infty}\frac{2}{j^2}\,\mathrm{K}_o\left[r\,\sqrt{v+j^2}\right]\left(\frac{\sin jl - \sin jd}{l-d}\right)\left(\frac{\sin jl' - \sin jd'}{l'-d'}\right)\right] \tag{27}$$

where $j = \pi k/m$, m is the aquifer thickness, $v = \imath\omega/D$, l and d are the upper and lower limits of the screened zone within the pumping well, respectively, and l' and d' are the upper and lower limits of the screened zone within the observation well, respectively.

Fig 3 presents the simulated amplitudes vs. distance and phase for pumping throughout the aquifer, from the upper half, and from the upper tenth. The solution is for an observation well that is screened in the upper tenth of the aquifer. In all cases, the multi-layer results are consistent with the partially and fully penetrating solutions. Note that amplitude decreases – and phase lag increases – with distance from the pumping well, and that the effect of partial penetration is to reduce the amplitude compared to the fully penetrating case.

For the second experiment, the leakance parameter ($L = K_v/m$) is reduced by a factor of ten, corresponding to anisotropic conditions (i.e., $\alpha = K_h/K_v = 10$, where α is the anisotropy ratio). The multi-layer solution can only be directly compared to the partially penetrating solution in an anisotropic aquifer when pumping is entirely horizontal (i.e., for a fully penetrating pumping well) because the partially penetrating analytic solution assumes isotropic conditions.

To allow comparison for a partially penetrating pumping well, an approximation is employed to vertically scale the aquifer so that it is isotropic. A standard method for converting an anisotropic aquifer to isotropic is to scale the aquifer thickness using $\zeta = \sqrt{\alpha}\,m$, where m is the original aquifer thickness and ζ is the scaled thickness (Bear, 1972). Thus, a layer thickness of $m = \sqrt{10}$ (instead of $m = 1$) is used in the partially penetrating case.

Fig 4 presents the simulated amplitudes as a function of distance and lag. Note that the multi-layer solution provides consistent results for most cases, with the only discrepancy being near the pumping well when only the top tenth of the aquifer is pumped. This discrepancy may be attributable to the scaling used in the partially penetrating case, meaning that the error lies in the inability of the partially penetrating solution to fully reproduce anisotropic conditions.

The final experiment assumes that the upper half of the aquifer (ℓ=6-10) has one tenth the hy-

draulic conductivity (both K_h and K_v) of the lower half (ℓ=1-5). Only one pumping scenario is used in this experiment; all pumping is from the lower half of the aquifer (ℓ=1-5). For the partially penetrating case, the lower-layer thicknesses are m=1, while the upper-layer thicknesses are m= $\sqrt{10}$. While this accounts for the vertical component of the hydraulic conductivity, K_v, it ignores the reduction in the horizontal component, K_h, which could affect the prediction accuracy.

Fig 5 presents the simulated amplitudes as a function of distance and lag for this experiment. Two monitoring intervals are displayed in the plot of amplitudes vs. distance; the lowermost and uppermost tenths (i.e., ℓ=1,10). Note that the behavior is consistent with the previous experiments, and also that amplitudes and lags display the anticipated behavior. Also note that the partially penetrating solution is consistent with the multi-layer solution, despite the fact that the horizontal conductivity within the upper layer is incorrectly modeled. This correspondence is likely due to the dominance of vertical flow over horizontal flow in the upper layer.

4 Application to the WIPP Site

The multi-layer aquifer solution is needed to interpret sinusoidal aquifer tests at Hydropad H-19 within the Waste Isolation Pilot Plant (WIPP) site, located near Carlsbad, NM, USA (Fig 6). The WIPP site is the home of the nation's first permanent nuclear repository, which lies 655 m below the ground surface in bedded, Permian-age halite deposits. These deposits are part of the Salado formation, which is composed of a sequence of thick evaporite beds overlain by the Rustler Formation.

The Culebra Dolomite Member is the most transmissive unit within the Rustler Formation in the vicinity of the WIPP site (Holt and Powers, 1988). WIPP characterization studies have shown that groundwater transport through the Culebra Dolomite would be the most significant pathway to the accessible environment if radionuclides are released from the repository through inadvertent human intrusion (USDOE, 1996).

Stratigraphic layering within the Culebra Dolomite changes little across WIPP, and can be subdivided into four units and two major hydrostratigraphic zones, the Upper Culebra and the Lower Culebra. Fractures in the Upper Culebra are predominantly gypsum filled with small vugs that occur parallel to the stratification. The Lower Culebra is more intensely fractured, has more vugs, and contains interbeds of poorly indurated dolomite. As a result, the Lower Culebra is generally several orders of magnitude more conductive than the Upper Culebra.

A total of 44 wells and four shafts penetrate the Culebra Dolomite on the 41.4 km^2 WIPP site. Aquifer testing facilities, called hydropads, have been installed across the WIPP site, with each hydropad consisting of a primary pumping well and multiple observation wells located at a range of distances from the pumping well. The purpose of the hydropads is to provide the capability to char-

acterize and monitor spatial and temporal hydrogeologic conditions at the site.

Sinusoidal Testing

Sinusoidal tests were conducted within the Culebra Dolomite between October 5 and November 12, 1995 at Hydropad H-19. The H-19 Hydropad (located at 32.3593°N, 103.7828°W) consists of seven wells that are normally used to monitor hydraulic head within the Culebra Dolomite. The Culebra Dolomite has a total thickness of m=7.4 m at this location, with the more-permeable Lower Culebra having a thickness of m_1=4.4 m, and the Lower Culebra having a thickness of m_2=3 m.

For site characterization purposes, two sinusoidal aquifer tests were conducted using Well b0 as the pumping well, with one test (Test 1) configured to pump from the Lower Culebra and a second test (Test 2) configured to pump from the Upper Culebra. A third sinusoidal test (Test 3) was conducted with pumping from the Lower Culebra interval within Well b4.

Pumping and observation wells were configured with straddle-packer systems designed to isolate the two intervals (i.e., the Upper and Lower Culebra) as well as the annulus above the Culebra Dolomite. All intervals were instrumented with gauge pressure transducers to measure the fluid pressure. Pumping well packer systems were configured to pump independently from either the upper or lower intervals.

Sinusoidal pumping was implemented using an electric, submersible, progressive cavity pump driven by a variable-frequency drive (VFD). The flow rate was monitored with inline magnetic flow meters. Flow was controlled using a proportional-integral-derivative (PID) feedback loop with the flow rate as the process variable and pump speed (VFD frequency output) as the control variable. The set point for the PID loop was programmed to vary using a sine function to produce the sinusoidal flow rates. The process variable flow rate was updated every second by the control computer to generate the sinusoidal signal. The pumping rate and all zone pressures were measured and logged at regular intervals. Data were collected and stored using an automatic data acquisition system. Additional information about conducting sinusoidal aquifer tests can be found in Young et al. (2002).

03

Tanmoy Das

Each sinusoidal test was preceded by a constant rate discharge period that introduced a recovery response during the sinusoidal portion of the tests. All tests were performed as net positive rate tests (due to hardware constraints and regulatory concerns), during which the pumping rate oscillated around a positive average flow rate (i.e., the sum of the constant-rate discharge test with the superimposed periodic signal).

Test conditions are shown in Table 1. The prior flow rate is the continuous rate during the period prior to switching over to a periodic test. The constant rate is the steady pumping during the periodic pumping test about which the periodic pumping oscillated. The periodic rate is added to the constant

rate at the amplitude and period indicated. The number of cycles during each test is also provided.

04

Tanmoy Das

Amplitude and Lag Estimation

While the amplitudes and phases of the process variables (Q, s) can be obtained by visually inspecting the pumping record and well hydrographs, visual estimation can be ambiguous when noise or an underlying trend are present. Multiple, linear regression using the ordinary least-squares (OLS) method is an alternative procedure for quantitatively estimating unknown coefficients, and is particularly useful for periodic functions.

OLS regression estimates of the pumping-rate amplitudes and phases were found using:

$$Q = Q_o + Q_1 \cos \omega t - Q_2 \sin \omega t \tag{28}$$

where Q is the observed pumping rate, ω is the prescribed pumping frequency, t is time, Q_o is the unknown, constant pumping rate during the test, and Q_1 and Q_2 are unknown coefficients used to find the pumping amplitude, $\mathcal{A}_Q = \sqrt{Q_1^2 + Q_2^2}$, and phase, $\mathcal{P}_Q = \arctan_2 (Q_2/Q_1)$, of the periodic component of the pumping rate.

A similar approach is used to determine drawdown amplitudes and phases:

$$s = s_o + s_1 \cos \omega t - s_2 \sin \omega t + \sum_{i=1}^{n} c_i f_i(t) \tag{29}$$

where s is the observed time series of drawdowns, s_o is a constant, s_1 and s_2 are the periodic responses at the known frequency in the well, and c_i and $f_i(t)$ are user-defined temporal trend coefficients and functions, respectively. Possible user-defined trend functions include $\ln(t)$, $1/t$, and t to account for recovery or persistent trends in the aquifer. Drawdown amplitudes, $\mathcal{A}_s = \sqrt{s_1^2 + s_2^2}$, and phases, $\mathcal{P}_s = \arctan_2 (s_2/s_1)$, are obtained from the regression coefficients.

Amplitudes and phases are estimated for all H-19 observation locations for the three sinusoidal tests. Recovery trend functions $\ln(t)$ and $1/t$ (i.e., the first two temporal terms in the Theis well function expansion) are included in the OLS regression because all sinusoidal tests were preceded by, and contemporaneous with, a constant-rate discharge test. Fig 7 illustrates the observed pumping rates and drawdown responses for Test 1, i.e., the H-19 Well b0 test in the Lower Culebra. Also shown are the regression fits to the observed data.

A spreadsheet utility was developed to facilitate the calculation of the amplitudes and lags of the periodic time series. The utility performs the OLS regression using observation-well and pumping-rate data to determine the amplitude and lags of the pumping signal. Given a sinusoidal signal from a pumping or observation well, the utility determines the coefficients for a series of linear equations. Note that the linear equations include the periodic components of the time-drawdown signal along

with user-specified trends. A summary of the installation and use of this utility is presented in Toll (2005), and is available from the authors.

Once the amplitudes and lags are determined, a unit amplitude, $\beta = \mathcal{A}_s/\mathcal{A}_Q$, is found by normalizing the drawdown amplitudes by the pumping-rate amplitude. The phase lag, $\tau = \mathcal{P}_s - \mathcal{P}_Q$, is found using the time delay between the drawdown and pumping-rate phases.

Fig 8 illustrates the anticipated amplitudes and lags for a two-layer aquifer. Note that the unit amplitude is greater in the more conductive, lower layer (β_l), and smaller in the upper layer (β_u). Also note that the lag is shorter in the lower layer (τ_l), and longer in the upper layer (τ_u). This behavior can be quantified using two additional parameters. The amplitude ratio, $\beta^* = \beta_u/\beta_l$, is the drawdown amplitude of the Upper relative to the Lower Culebra. The lag, $\tau^* = \tau_u - \tau_l$, is the time delay between the Upper and Lower Culebra.

Parameter Estimation

Preliminary estimates of the hydraulic properties (D, T, S) for each well were found using the single-layer, confined aquifer solution. While the single-layer solution does not explicitly account for the multi-layer nature of the aquifer system nor the fact that pumping was not conducted across both layers, it can provide an initial estimate of the hydraulic properties in the vicinity of each well. Given the amplitude and phase lag of the pumping rate and observation well signal, the aquifer hydraulic properties were calculated using the method presented in Rasmussen et al. (2003). A second spreadsheet utility was developed to implement this inverse procedure (Toll, 2005), and is available from the authors.

A more robust analysis of this multi-layer system was performed using the multi-layer analytic solution. The system is conceptualized as a more conductive unit underlying a less conductive unit, with no-flow boundaries above and below the system, and infinite areal extent. Both units were subdivided into ten layers, each of equal thickness. The hydraulic heads within the Upper and Lower Culebra units were calculated as the arithmetic mean of the heads within each unit. The Lower Culebra is assumed to have uniform hydraulic properties (D, T, S, L), while the hydraulic properties within the Upper Culebra are segregated into two zones (Zones 1 and 2).

Rather than using the multi-layer solution in a forward sense (i.e., using aquifer parameters to predict drawdown), our objective is the inverse (i.e., estimate parameters using observed drawdowns). For this application, aquifer hydraulic properties were estimated using the Nelder-Mead simplex search method (Nelder and Mead, 1965), which is a multi-dimensional, unconstrained, nonlinear, minimization technique. The Nelder-Mead method requires the specification of an objective function, which is minimized.

The objective function used to obtain the multi-layer aquifer parameters is defined using the sum of squared errors for both the amplitudes and lags in the pumping and non-pumping layers:

$$\epsilon^2 = \sum_{j=1}^{4} \sum_{i=1}^{6} \epsilon_j^2(i) \tag{30}$$

where i corresponds to each of the six observation wells and j corresponds to each of the four error components; $\epsilon_1 = \hat{\beta}/\beta - 1$ is the unit amplitude error in the lower, more-conductive unit, $\epsilon_2 = \hat{\tau} - \tau$ is the phase lag error in the lower unit, $\epsilon_3 = \hat{\beta}^* - \beta^*$ is the amplitude ratio error in the upper unit, $\epsilon_4 = \hat{\tau}^* - \tau^*$ is the phase difference error in the upper unit, and $\hat{\cdot}$ indicates the fitted value.

Six aquifer parameters were estimated; the transmissivity and diffusivity for the Lower Culebra plus the two zones within the Upper Culebra. Aquifer storativity was calculated using the transmissivity-diffusivity ratio, $S = T/D$. Initial parameter estimates were provided by the single-layer confined solution.

Results and Discussion

Table 2 presents the estimated amplitudes and lags for the pumping rates, Q, and drawdowns, s, for both the Lower and Upper Culebra intervals for all pumping tests. All tests yield similar unit amplitudes, β, for the same observation interval at similar distances in the Lower Culebra. The effect of distance is also evident - greater distances from the pumping well are associated with lower unit amplitudes.

Table 2 also presents the estimated aquifer hydraulic parameters using the single-layer assumption. Note that the diffusivities, transmissivities, and storativities are similar regardless of whether the Upper Culebra is pumped at Well b0 or when the Lower Culebra is pumped at either Well b0 or b4.

Yet, two types of amplitude ratios, β^*, and phase differences, τ^*, are apparent in the Upper Culebra. Wells b0, b2, b3, and b7 have larger amplitude ratios and smaller phase differences when compared with wells b4, b5, and b6. This behavior may be due to geologic factors, in that the first set of wells lie to the east and south of the pumping well, b0, while the second set lie to the north and west.

This same trend is observed during the third test (i.e., when Well b4, located to the north and west of the observation wells, is pumped), except that Well b0 now joins the set of wells with larger unit amplitudes and phase lags. Using these observations, we assign Wells b0, b2, b3, and b7 to Zone 1, and Wells b4, b5, and b6 to Zone 2.

Tests 1 and 3 were used to demonstrate the application of the multi-layer solution. Both tests were conducted using pumping in the Lower Culebra, with pumping from Wells b0 and b4, respectively.

Data from Test 2 were not used for optimization because the optimization procedure was unable to match the observed phase lags in this less conductive unit.

The relationship between distance and the unit amplitude and the phase lag in the Lower Culebra are shown in Fig 9. Observed data for the three tests are shown, along with forward model results for the single-layer solution as well as for Zones 1 and 2 using the multi-layer solution. Note that the unit amplitude decreases, while the phase lag increases, with increasing distance. No substantial difference between the unit amplitude and phase lags between the three tests is observed.

Note also that model fits to the data are relatively similar, and that the multi-layer predictions for the unit amplitude in both Zones 1 and 2 are indistinguishable from each other. This indicates that the effects of spatial variability within the Upper Culebra minimally affects amplitudes within the Lower Culebra. A small phase difference can be seen, however, with a small delay for Zone 1 relative to Zone 2. It is also interesting to note that the single-layer model provides an equally reasonable fit to the observations.

Fig 9 also presents the amplitude ratio and phase difference between the Upper and Lower Culebra for each observation well. The amplitude ratio is calculated as the unit amplitude of the Lower Culebra divided by the unit amplitude of the Upper Culebra. The phase difference is calculated as the phase lag of the Lower Culebra subtracted from the phase lag of the Upper Culebra. Amplitude ratios are always less than one, which means that the amplitude of fluctuations within the Lower Culebra are always greater than in the Upper Culebra.

Note that two amplitude ratio behaviors are apparent, a ratio larger than 0.6 (i.e., the Upper Culebra amplitude is greater than 60 percent of the Lower Culebra amplitude at the same distance) in Zone 1, while Zone 2 displays a much lower ratio, less than 14%. No clear trend with distance is observed for observed ratios. Model predictions show a constant amplitude ratio except near the pumping well. While model predictions for the amplitude ratio provide a reasonable fit for Zone 2, they lie slightly above the observed data for the more-conductive Zone 1.

Fig 9 also shows the phase difference between the two layers. Note that the phase differences are always positive, which implies that the Upper Culebra always lags behind the Lower Culebra, even when the Upper Culebra is pumped (i.e., Test 2). Also note that the lag difference is less for those wells with a higher amplitude ratio, but the difference is greater for wells with a smaller amplitude ratio. No clear trend with distance is obvious for the lag differences, which is consistent with model predictions.

Table 3 presents average hydraulic properties using the single-layer approach applied to all wells and all tests. The arithmetic-mean transmissivity for the Lower Culebra of T=7.52($\pm$0.20)$\times10^{-6}$ m^2/s compares favorably to the estimated value of T=6.8$\times10^{-6}$ m^2/s previously estimated at the

H-19 Hydropad (Beauheim and Ruskauff, 1998).

The arithmetic-mean hydraulic diffusivity of the Lower Culebra estimated using the single-layer assumption is D=1.72($\pm$0.11) m^2/s, and the corresponding mean storativity is S=4.56($\pm$0.30)$\times10^{-6}$. These estimates are comparable to previous results using early time drawdown data (D=0.99 m^2/s, S=6.9$\times10^{-6}$), but differ by an order of magnitude from late-time data (D=0.14 m^2/s, S=49$\times10^{-6}$). The better correspondence between aquifer hydraulic parameters estimated using sinusoidal aquifer tests and those estimated using early time (as opposed to late-time) data from conventional aquifer test was previously noted in Rasmussen et al. (2003).

Table 3 summarizes aquifer hydraulic properties for the two-layer model. The estimated diffusivity of the Lower Culebra using the two-layer model, D=1.67 m^2/s, compares favorably with the single-layer model, D=1.72 m^2/s. Also, the reported full Culebra transmissivity of T=6.8$\times10^{-6}$ m^2/s (Beauheim and Ruskauff, 1998) compares favorably with the two-layer transmissivity for the Lower Culebra of T=6.73$\times10^{-6}$ m^2/s, as well as with the single-layer estimate of T=7.52$\times10^{-6}$ m^2/s found in the previous section. The contribution by the Upper Culebra to the total transmissivity can be neglected due to its magnitude.

The reported geometric mean core hydraulic conductivity of the Upper Culebra is K=0.83$\times10^{-9}$ m/s (Meigs and Beauheim, 2001), which corresponds to a transmissivity of T=2.5$\times10^{-9}$ m^2/s. This value lies within the interval (T=1.08$\times10^{-9}$ to 16.1$\times10^{-9}$ m^2/s) estimated for the two Upper Culebra zones. Diffusivities within the Upper Culebra are also variable, ranging between D=96.3$\times10^{-6}$ to 16.8$\times10^{-3}$ m^2/S.

While the transmissivity estimates are consistent with previous results, both the single- and two-layer storativities (and diffusivities) are not, tending to underestimate the previously estimated storativity (and overestimate the diffusivity) by an order of magnitude using late-time data, and less using early-time data. This discrepancy can likely be attributed to the known, dual-porosity nature of the aquifer, which yields a smaller, early-time storativity followed by a larger, later-time storativity.

Because the periodicity of the sinusoidal test is shorter than the duration of a conventional test, the resulting sinusoidal parameter estimate likely represents the early-time secondary porosity, while the conventional test represents the later-time total porosity. The fact that the storativity found here approaches the early-time storativity found previously (Beauheim and Ruskauff, 1998) supports this interpretation. This interesting result is similar to that shown in (Rasmussen et al., 2003) in which the storatavity of an unconfined aquifer was much smaller during the sinusoidal test than the value estimated using a conventional test. The solution to periodic pumping in dual-porosity media that might be used to confirm this interpretation is not presently available.

5 Summary and Conclusions

This work presents the forward solution to sinusoidal flow in a multi-layer aquifer. This solution provides the capability to account for variations in material properties and pumping rates within a vertical section. It stops short of providing a direct inverse analytical solution to determine aquifer parameters from observation data. Instead, an iterative least-squares optimization method is used to estimate aquifer hydraulic properties. The approach uses unit amplitudes and phase lags to characterize the hydraulic response to sinusoidal pumping. These values are directly related to the transmissivity of the aquifer layers, along with their hydraulic diffusivity, thickness, distance from the pumping well, and pumping frequency.

Simulations using a synthetic aquifer setting are used to study the multi-layer solution behavior for different material properties. For a situation where a homogeneous two-layer aquifer is pumped in one layer, the solution is equivalent to the partially penetrating solution. The multi-layer solution is applied to a two-layer system where each layer is divided into ten sublayers of equal thickness and well discharge. This means that the boundary condition along the well screen is uniform inflow over the vertical. This assumption facilitates comparison to the partially penetrating solution, which also specifies a uniform inflow.

The sinusoidal approach is demonstrated using data from three aquifer hydraulic tests that monitored drawdown responses in two layers (the Lower and Upper Culebra) at the Waste Isolation Pilot Plant, located near Carlsbad, NM. The estimated transmissivity of the more-conductive layer (Lower Culebra) using single- and multi-layer sinusoidal solutions are consistent with estimates obtained from previous aquifer hydraulic testing. In addition, the estimated transmissivity of the less-conductive layer (Upper Culebra) is consistent with the transmissivity obtained using the average hydraulic conducitivity of rock cores.

The hydraulic properties of the more-conductive Lower Culebra are spatially uniform, which is consistent with previous testing. The less-conductive Upper Culebra, however, displays distinct differences. One zone, consisting of four wells to the east and south of the pumping well, has larger amplitude ratios and smaller phase differences when compared with three wells in a second zone that lies to the north and west. It is plausible that geologic variation is a factor in this behavior.

Phase lags observed during pumping from the less conductive unit are identical with those when the more conductive unit is pumped, which is inconsistent with model results which indicate that a significant, additional lag should occur. The system appears to behave as though pumping is directly from the Lower Culebra, even though pumping was from the Upper Culebra. This may be due to localized fractures near the pumped borehole that provides preferential connectivity between the two units.

While the model captures the dominant behavior of the sinusoidal response, the model does not fully reproduce the response in the less-conductive, Upper Culebra unit. Reasons for the inability to perfectly match the observed data may be the failure to account for known dual porosity conditions and spatial heterogeneity within these low permeability units, as well as the assumption that observed drawdowns are the arithmetic average of hydraulic head within the layer, which neglects the possible influence of more permeable sublayers dominating the borehole response.

The estimated storativity, however, was found to be an order-of-magnitude smaller than previous estimates. This finding is consistent with Rasmussen et al. (2003) which showed that sinusoidal testing of an unconfined aquifer provides an early-time estimate of storativity, while conventional tests commonly provide a late-time estimate. In this case, the early-time storativity estimate is consistent with the dual-porosity nature of the aquifer, and likely represents the secondary porosity. Thus, aquifer properties found using sinusoidal testing are consistent with the prevailing understanding of the hydrostratigraphic conditions at this site.

Further evaluation of the effects of storage to consider dual-porosity behavior using the observed amplitude-phase lag supports a single-porosity interpretation, i.e., instantaneous release from storage. While this does not preclude the presence of a dual-porosity system, it suggests that a smaller frequency (i.e., longer pumping period) may be required to induce release of water from storage within inclusions.

Acknowledgments. This research was partially supported by funding from WIPP programs administered by the Office of Environmental Management of the U.S. Department of Energy. Sandia is a multiprogram laboratory operated by Sandia Corporation, a Lockheed Martin Company, for the United States Department of Energy's National Nuclear Security Administration under contract DE-AC04-94AL85000.

References

Abramovitz M, IA Stegun (1972) *Handbook of mathematical functions*, Dover, New York NY.

Bakker M (2004) "Transient analytic elements for periodic Dupuit-Forchheimer flow", *Advances in Water Resources*, 27(1):3-12.

Bakker M (2009) "Sinusoidal pumping of groundwater near cylindrical inhomogeneities", *Journal of Engineering Mechanics*, 64:131-143, doi 10.1007/s10665-008-9244-0.

Bear J (1972) *Dynamics of fluids in porous media*, Dover, New York NY.

Beauheim RL, GJ Ruskauff (1998) *Analysis of hydraulic tests of the Culebra and Magenta Dolomites*

and Dewey Lake Redbeds conducted at the Waste Isolation Pilot Plant site, Sandia National Laboratories, SAND98-0049, Albuquerque NM.

Black JH, KL Kipp Jr (1981) "Determination of hydrogeological parameters using sinusoidal pressure tests: A theoretical appraisal", *Water Resources Research*, 17(3):686-692.

Bruggeman GA (1966) "Analyse van de bodemconstanten in een grondpakket, bestaande uit twee of meer watervoerende lagen gescheiden door semi-permeabele lagen". Unpublished research report, cited in Kruseman GP, NA de Ridder (1991), *Analysis and Evaluation of Pumping Test Data* Second edition, International Institute for Land Reclamation and Improvement, ILRI Publication 47, Wageningen, The Netherlands.

Bruggeman GA (1999) *Analytical solutions of geohydrological problems*, Developments in Water Science, #46, Elsevier.

Carr PA, GS van der Kamp (1969) "Determining aquifer characteristics by the tidal method", *Water Resources Research*, 5(1):1023-1031.

Haborak KG (1999) *Analytical solutions to flow in aquifers during sinusoidal aquifer pump tests*, MS Thesis, University of Georgia, Athens GA 30602.

Hemker CJ (1999) "Transient well flow in vertically heterogeneous aquifers", *Journal of Hydrology*, 225(1-2):1-18.

Hemker CJ, C Maas (1987) "Unsteady flow to wells in layered and fissured aquifer systems", *Journal of Hydrology*, 90(3-4):231-249.

Holt RM (1997) *Conceptual model for transport processes in the Culebra Dolomite member, Rustler formation*, Sandia National Laboratories, SAND97-0194, Albuquerque NM.

Holt RM, DW Powers (1988) *Facies variability and post-depositional alteration within the Rustler Formation in the vicinity of the Waste Isolation Pilot Plant, southeastern New Mexico*, Department of Energy, WIPP-DOE-88-004, Carlsbad NM.

Javandel I, PA Witherspoon (1983) "Analytical solution of a partially penetrating well in a two-layer aquifer", *Water Resources Reseasrch*, 19(2):567-578.

Maas C (1986) "The use of matrix differential calculus in problems of multiple-aquifer flow", *Journal of Hydrology*, 99(1-2):43-67.

Maas C (1987) "Groundwater-flow to a well in a layered porous medium, 1. Non-steady multiple-aquifer flow", *Water Resources Research*, 23(8):1683-1688.

Meigs LC, RL Beauheim (2001) Tracer tests in a fractured dolomite, 1. Experimental design and observed tracer recoveries. *Water Resour. Res.*, *37*(5):1113-1128.

Mercer JW, DL Cole, RM Holt (1998) *Basic data report for drillholes on the H-19 Hydropad (Waste Isolation Pilot Plant - WIPP)*, Sandia National Laboratories, SAND98-0071, Albuquerque NM.

Nelder JA, R Mead (1965) "A simplex method for function minimization", *Computer Journal*, 7(4):308-313.

Neuman SP, PA Witherspoon (1969a) "Theory of flow in a confined two aquifer system", *Water Resources Research*, 5(4):803-816.

Neuman SP, PA Witherspoon (1969b) "Applicability of current theories of flow in leaky aquifers", *Water Resources Research*, 5(4):817-829.

Rasmussen TC, KG Haborak, MH Young (2003) "Estimating aquifer hydraulic properties using sinusoidal pumping at the Savannah River site, South Carolina, USA", *Hydrogeology Journal*, 2003(11):466-482, doi 10.1007/s10040-003-0255-7.

Streltsova TD (1988) *Well testing in heterogeneous formations*, Exxon Monographs, John Wiley & Sons.

Sun H (1997) "A two-dimensional analytical solution of groundwater response to tidal loading in an estuary", *Water Resources Research*, 33(6):1429-1435.

Tang Z, JJ Jiao (2001) "A two-dimensional analytical solution for groundwater flow in a leaky confined aquifer system near open tidal water", *Hydrological Processes*, 15:573-585, doi 10.1002/hyp.166.

Toll NJ (2005) *Barometric fluctuation removal in water level records and solutions to flow in aquifers during sinusoidal aquifer pumping tests*, MS Thesis, University of Georgia, Athens GA 30602.

Townley LR (1995) "The response of aquifers to periodic forcing", *Advances in Water Resources*, 18(3):125-146.

Trefry MG (1999) "Periodic forcing in composite aquifers", *Advances in Water Resources*, 22(6):646-656.

US DOE (1996) *Title 40 CFR 191 compliance certification application for the Waste Isolation Pilot Plant*, U.S. Department of Energy, DOE/CAO-1996-2184, Carlsbad Area Office, Carlsbad NM.

Young MH, TC Rasmussen, FC Lyons, KD Pennell (2002) "Optimized system to improve pumping rate stability during aquifer tests", *Ground Water*, 40(6):629-637.

List of Tables

Table 1: Sinusoidal aquifer test conditions at WIPP Site H-19.

	Test 1	Test 2	Test 3
Test Identifier	H190CA49	H190CA47	H194CA06
Pumping Well	b0	b0	b4
Unit Pumped	Lower	Upper	Lower
Pumping Rate (Lpm)			
Prior rate[a]	10.7	3.65	10.7
Constant rate[b]	6.3	2.7	6.3
Periodic rate	4.4	0.8	4.4
Total Cycles	7	7	6
Period (hrs/cycle)	1	1	1

[a] Nonperiodic pumping rate prior to sinusoidal aquifer test.

[b] Nonperiodic pumping rate during sinusoidal aquifer test, upon which the periodic rate is superimposed.

Table 2: WIPP Site H-19 sinusoidal aquifer test results, showing distance from pumping well (r), unit amplitudes (lower unit, β_l; upper unit, β_u; ratio between units, β^*), phase lags (lower unit, τ_l; upper unit, τ_u, difference between units, τ^*), and single-layer parameters (diffusivity, D; transmissivity, T; storativity, S).

Well	Test	r (m)	β_l (s/m^2)	β_u (s/m^2)	β^* (-)	τ_l (radians)	τ_u (radians)	τ^* (radians)	D (m^2/s)	T (m^2/s)	S (-)
b0	3	22.31	16,753	12,714	0.759	0.876	1.009	0.133	1.452	7.12×10^{-6}	4.90×10^{-6}
b2	1	25.07	15,766	13,591	0.862	0.938	1.137	0.199	1.498	6.84×10^{-6}	4.56×10^{-6}
	2	25.07	15,435	13,148	0.852	0.943	1.147	0.204	1.477	6.98×10^{-6}	4.73×10^{-6}
	3	40.15	7,527	6,568	0.873	1.397	1.595	0.198	1.286	7.25×10^{-6}	5.64×10^{-6}
b3	1	11.02	31,670	20,938	0.661	0.504	0.847	0.343	2.314	7.62×10^{-6}	3.30×10^{-6}
	2	11.02	30,119	25,153	0.835	0.523	0.785	0.262	2.006	7.68×10^{-6}	3.83×10^{-6}
	3	32.52	12,560	9,753	0.777	1.008	1.291	0.283	2.049	7.69×10^{-6}	3.75×10^{-6}
b4	1	22.31	17,008	1,202	0.071	0.826	1.744	0.918	1.739	7.64×10^{-6}	4.39×10^{-6}
	2	22.31	16,214	1,645	0.101	0.833	1.942	1.109	1.693	7.91×10^{-6}	4.67×10^{-6}
b5	1	13.82	26,358	2,513	0.095	0.668	1.593	0.925	1.319	6.54×10^{-6}	4.96×10^{-6}
	2	13.82	25,366	3,535	0.139	0.669	1.684	1.015	1.313	6.79×10^{-6}	5.17×10^{-6}
	3	16.05	21,566	1,706	0.079	0.781	1.724	0.943	1.070	6.51×10^{-6}	6.08×10^{-6}
b6	1	19.89	18,131	1,488	0.082	0.680	2.660	1.980	2.567	9.29×10^{-6}	3.62×10^{-6}
	2	19.89	17,276	2,113	0.122	0.687	2.438	1.751	2.480	9.62×10^{-6}	3.88×10^{-6}
	3	25.83	15,661	994	0.063	0.819	3.000	2.181	2.390	8.39×10^{-6}	3.51×10^{-6}
b7	1	12.19	27,846	21,892	0.786	0.598	0.819	0.221	1.498	7.09×10^{-6}	4.74×10^{-6}
	2	12.19	26,538	22,223	0.837	0.615	0.814	0.199	1.258	7.19×10^{-6}	5.30×10^{-6}
	3	29.97	11,924	9,275	0.778	1.083	1.311	0.228	1.419	7.21×10^{-6}	5.08×10^{-6}

Table 3: Summary of WIPP Site H-19 aquifer hydraulic properties.

Aquifer - Method	Diffusivity D (m^2/s)	Transmissivity T (m^2/s)	Storativity S (-)
Lower Culebra			
Previous Studies[a]			
Early-Time	0.99	6.8×10^{-6}	6.9×10^{-6}
Late-Time	0.14	6.8×10^{-6}	$49.\times10^{-6}$
Single Layer Inverse[b]	1.72	7.52×10^{-6}	4.56×10^{-6}
	(0.11)	(0.20×10^{-6})	(0.18×10^{-6})
Two Layer (all wells)	1.67	6.73×10^{-6}	4.05×10^{-6}
Upper Culebra			
Previous Studies[c]	-	2.5×10^{-9}	-
Two Layer			
Zone 1 (b0, b2, b3, b7)	16.8×10^{-3}	16.1×10^{-9}	0.96×10^{-6}
Zone 2 (b4, b5, b6)	96.3×10^{-6}	1.08×10^{-9}	11.1×10^{-6}

[a] Diffusivity calculated using $D = T/S$, from Beauheim and Ruskauff (1998).

[b] Values are arithmetic average of all tests, standard error of the mean in parentheses.

[c] Transmissivity calculated using $T = mK$, where m is the layer thickness (3 m), and K is the hydraulic conductivity of core samples, from Meigs and Beauheim (2001).

List of Figures

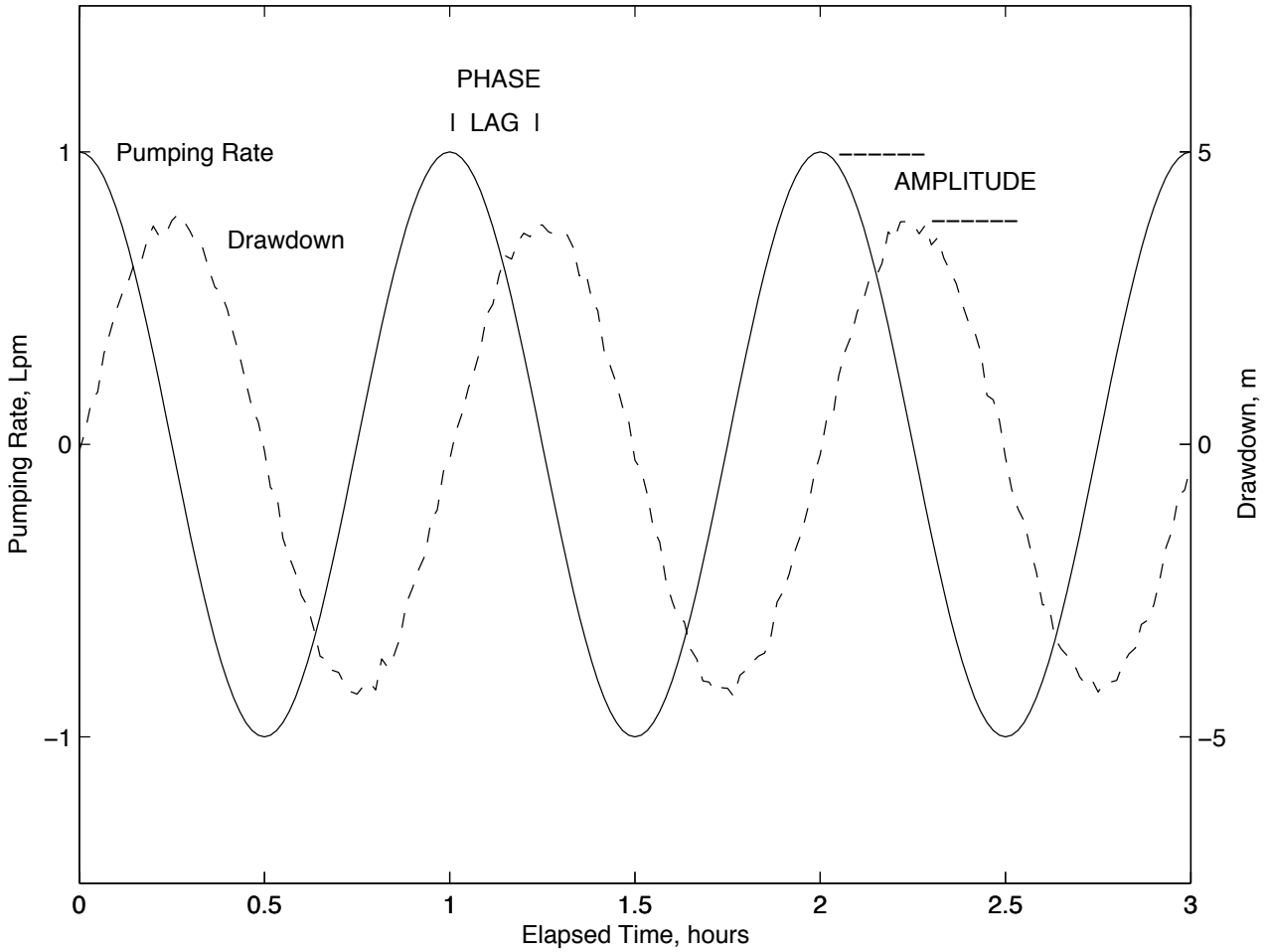

Figure 1: Diagram of sinusoidal aquifer test showing pumping rate (solid line) and drawdowns in observation wells (broken lines).

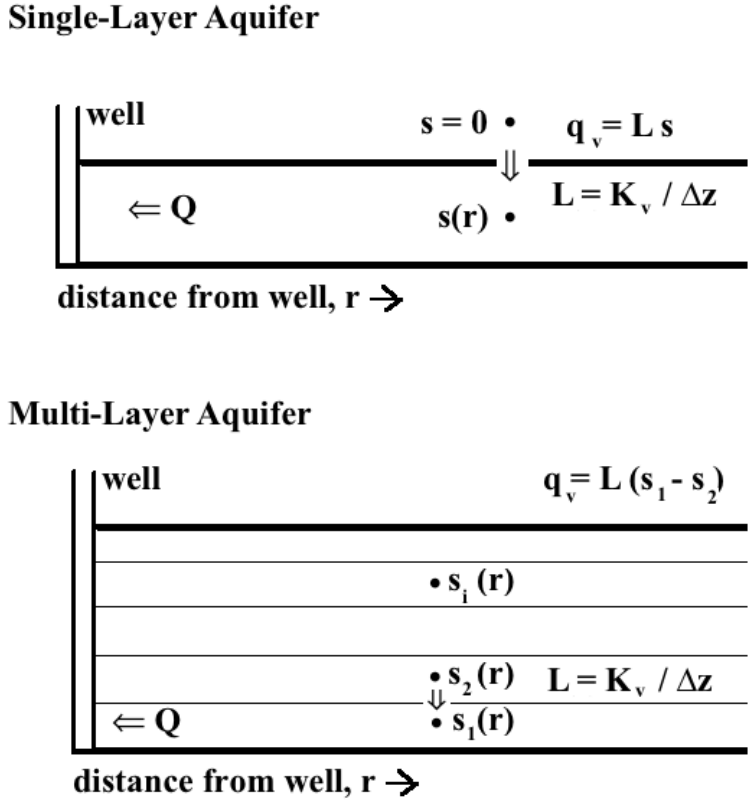

Figure 2: Diagram of single- and multi-layer aquifers showing conceptualization of vertical flux, q_v, away from the pumping well. In a single-layer aquifer, the leakage, L, is only a function of the drawdown within the aquifer; no drawdown is observed outside of the aquifer. In a multi-layer aquifer, the leakage is a function of the hydraulic gradient between the layers.

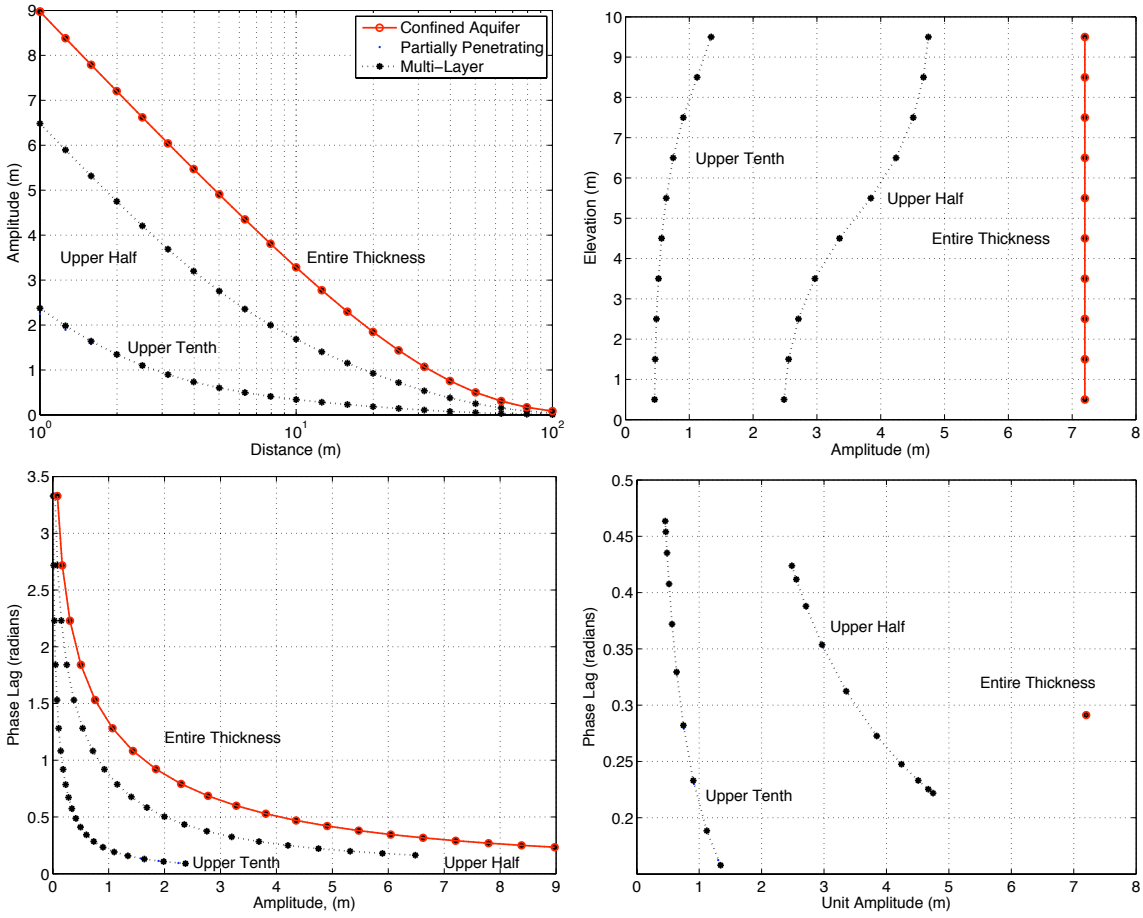

Figure 3: Comparison of single-layer (red), partially penetrating (blue), and multi-layer (black) analytic solutions for a sinusoidal pumping rate in a homogeneous, isotropic aquifer. Single-layer solution assumes uniform pumping throughout the full aquifer thickness. Partially penetrating and multi-layer solutions assume pumping from a) the entire thickness, b) the upper half, and c) the upper tenth of the aquifer. Amplitudes vs. distance (upper left) and phase lag (lower left) assume observation interval is in upper tenth of aquifer. Amplitudes vs elevation (upper right) and phase lag (lower right) as a function of elevation assume observation interval is two meters from the pumping well.

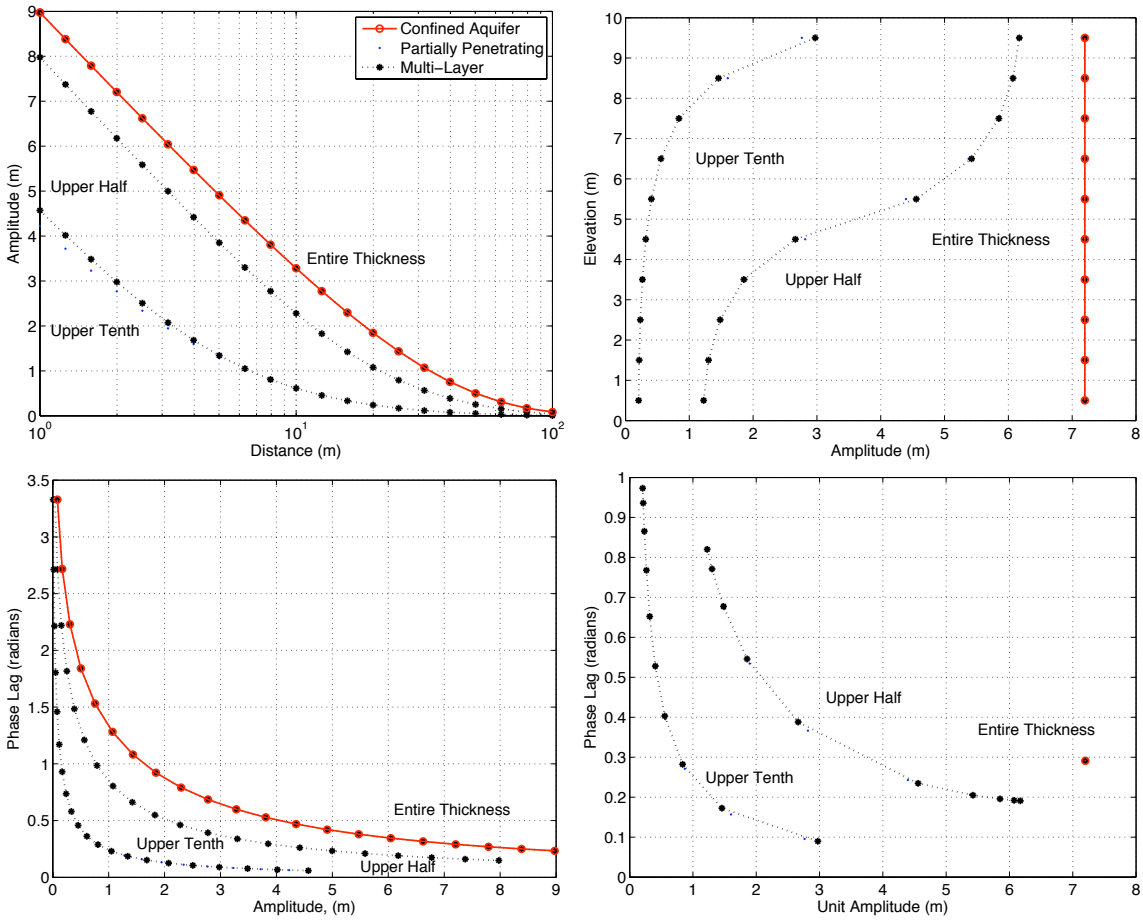

Figure 4: Comparison of single-layer (red), partially penetrating (blue), and multi-layer (black) analytic solutions for a sinusoidal pumping rate in a homogeneous, anisotropic aquifer with anisotropy ratio ($\alpha = K_h/K_v$) of ten. Partially penetrating solution obtained by scaling elevation by $\sqrt{\alpha}$. The single-layer solution assumes uniform pumping throughout the full aquifer thickness. Partially penetrating and multi-layer solutions assume pumping from a) the entire thickness, b) the upper half, and c) the upper tenth of the aquifer. Amplitudes vs. distance (upper left) and phase lag (lower left) assume observation interval is in upper tenth of aquifer. Amplitudes vs elevation (upper right) and phase lag (lower right) as a function of elevation assume observation interval is two meters from the pumping well.

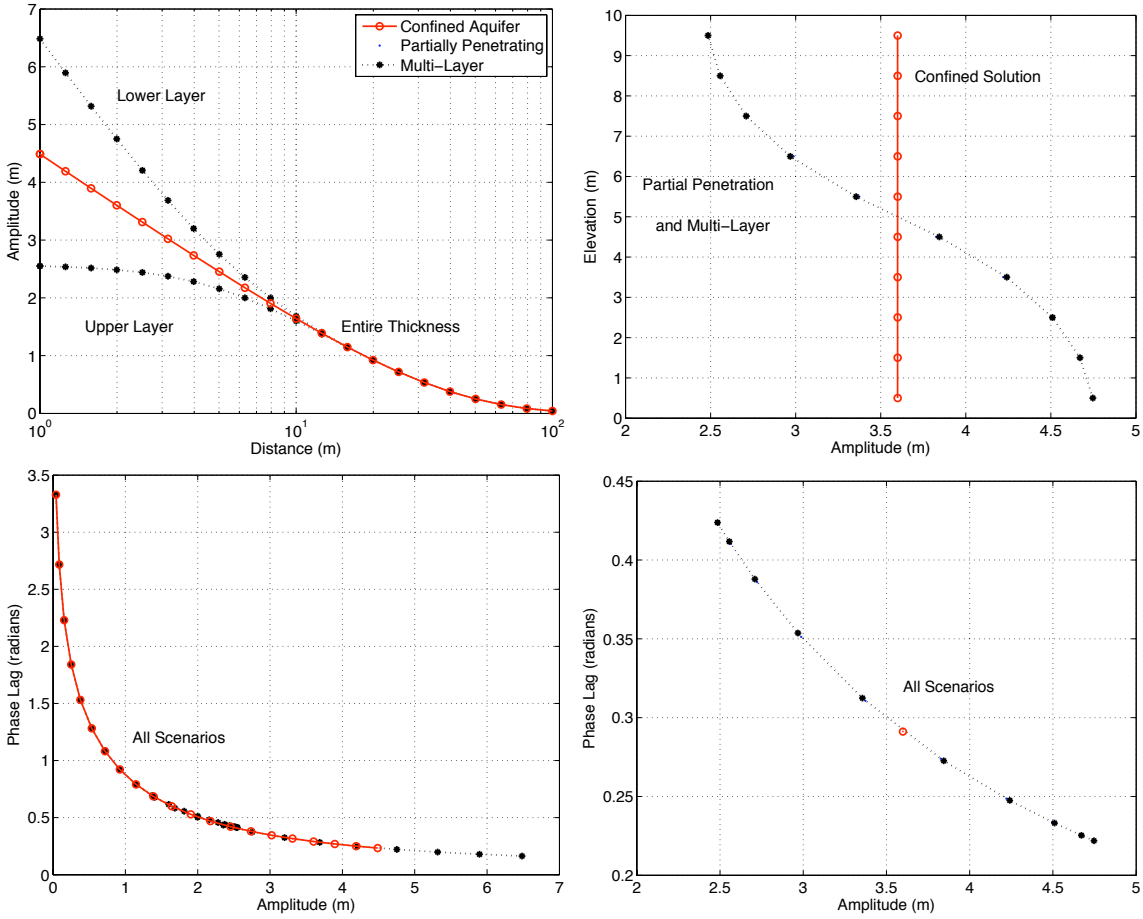

Figure 5: Comparison of single-layer (red), partially penetrating (blue), and multi-layer (black) analytic solutions for sinusoidal pumping in a two-region aquifer, with the upper region having one-tenth the hydraulic conductivity of the lower region, and with pumping entirely from the lower region in all scenarios. Amplitudes in uppermost and lowermost layers vs. distance (upper left) and phase lag (lower left). Amplitudes vs elevation (upper right) and phase lag (lower right) as a function of elevation assume observation interval is two meters from the pumping well.

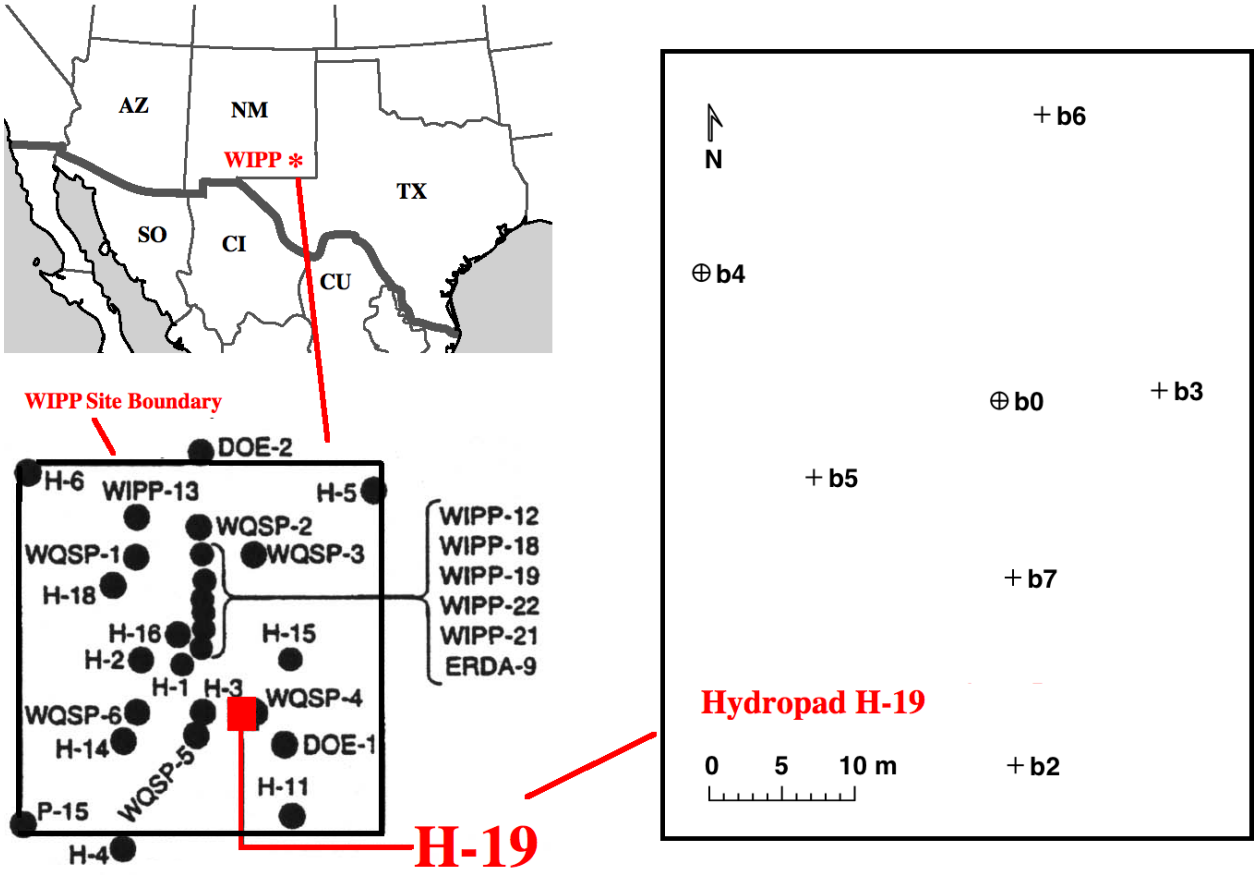

Figure 6: WIPP site location map showing well positions at WIPP Hydropad H-19. Sinusoidal aquifer Test 1 conducted at Well b0, Lower Culebra. Test 2 conducted at Well b4, Lower Culebra. Test 3 conducted at Well b0, Upper Culebra.

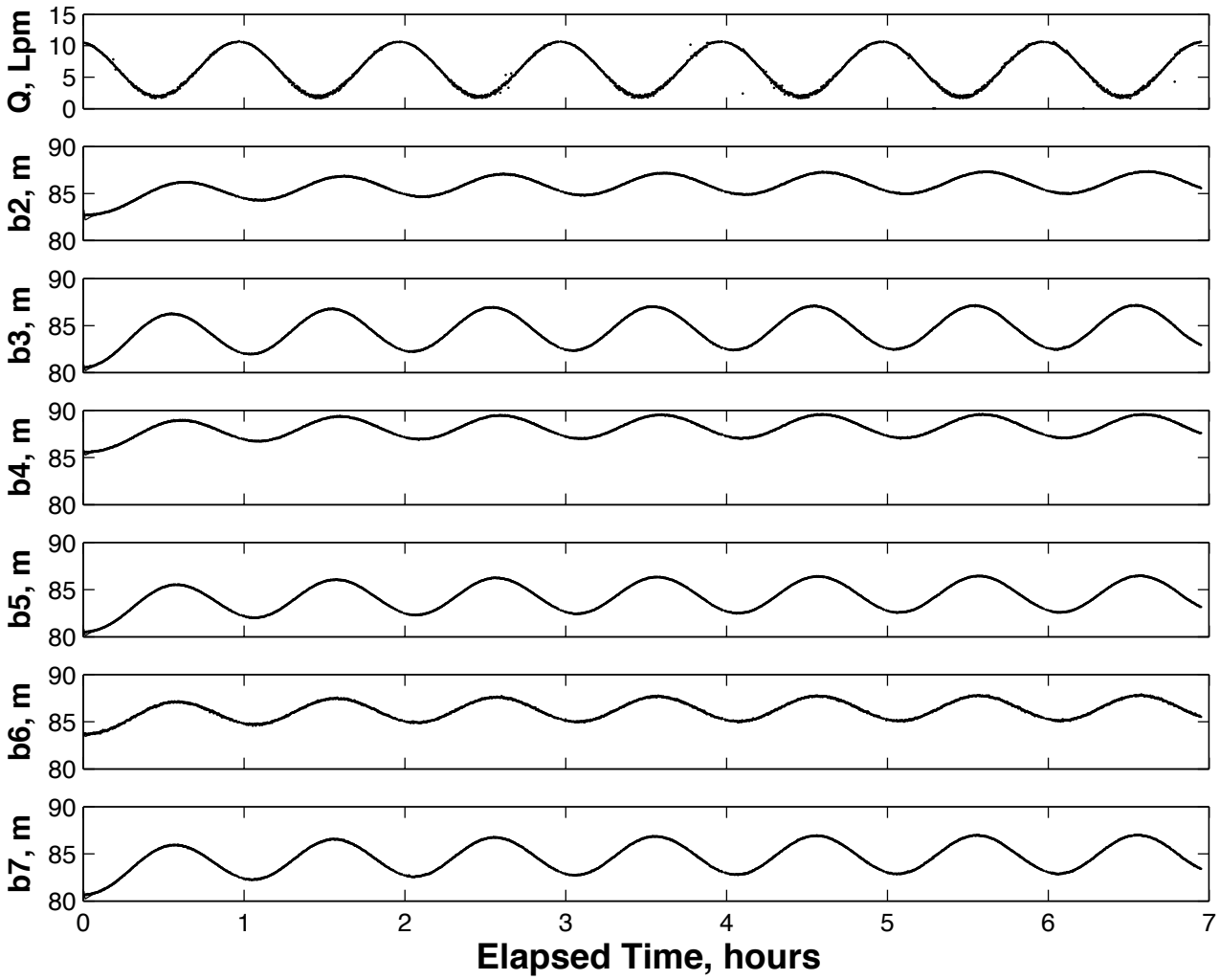

Figure 7: Observed and fitted pumping rate and Lower Culebra pressure heads for Test 1 (WIPP Hydropad H-19 Well b0, Lower Culebra pumping). Observed data is represented by black dots, least-squares fit represented by solid line, which is indistinguishable from the data.

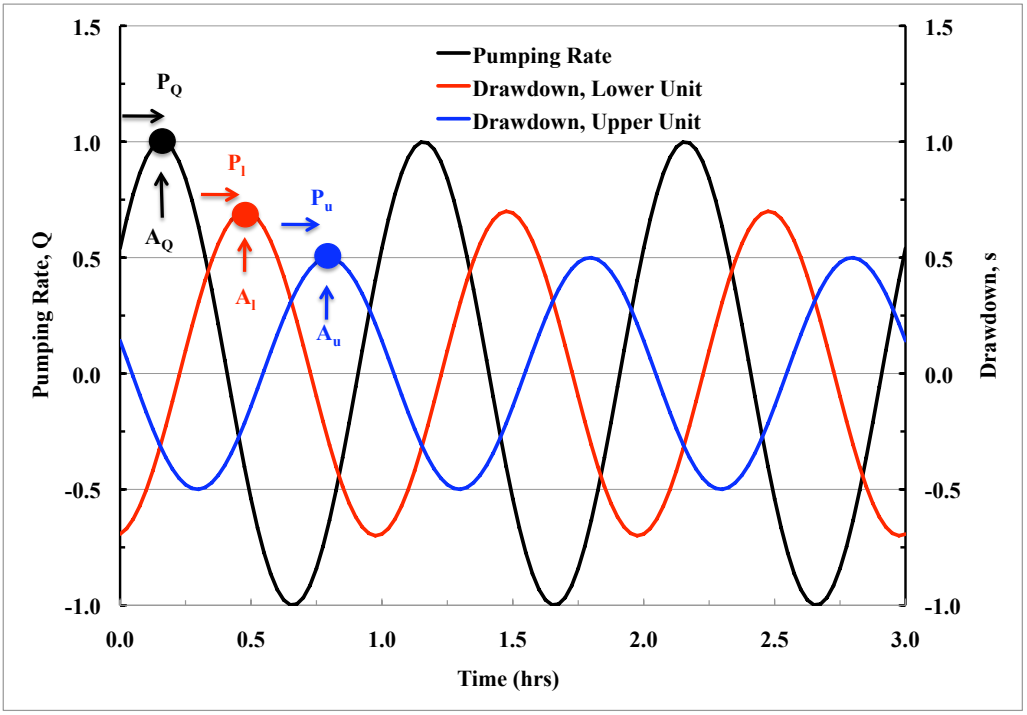

Figure 8: Conceptual diagram of sinusoidal aquifer test showing pumping rate (black) and observed drawdowns in the lower (red) and upper (blue) units. Also shown are the amplitudes (A_Q, A_l, A_u) and phase lags (P_Q, P_l, P_u) for the pumping rate and observed drawdowns.

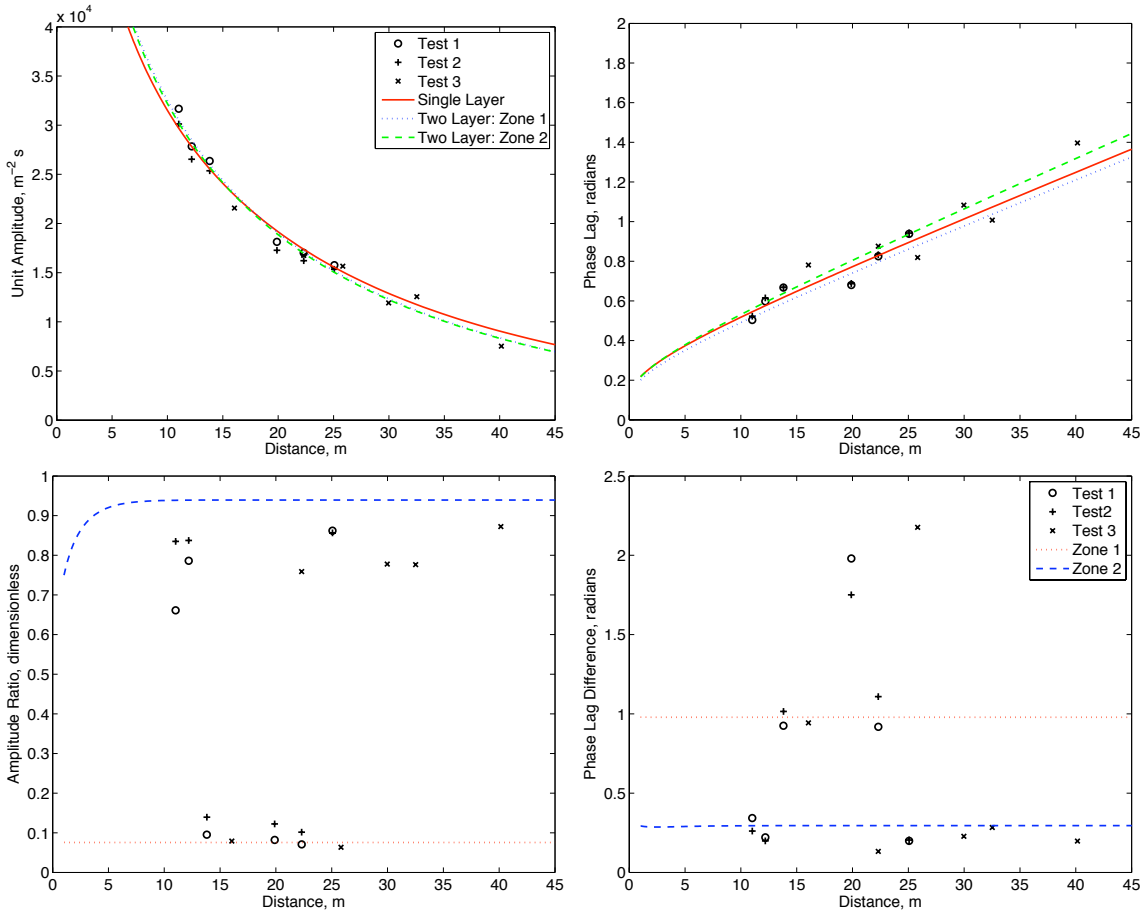

Figure 9: Observed amplitudes and phase lags vs distance for WIPP Hydropad H-19 observation wells in response to sinusoidal pumping. Unit amplitudes (upper left) and phase lags (upper right) for the Lower Culebra relative to the pumping well. Amplitude ratios (lower left) and phase differences (lower right) shown for Upper Culebra relative to the Lower Culebra. Also shown is the single-layer solution assuming horizontal flow in the Lower Culebra only, along with the predicted responses in two zones for the multi-layer aquifer solution.

Sinusoidal Hydraulic Testing of a Multi-Layer Aquifer at the Waste Isolation Pilot Plant , Carlsbad , NM , USA

Rasmussen, Todd C; Toll, Nathanial J; Bakker, Mark

01 Tanmoy Das Page 2
6/2/2019 18:00

02 Tanmoy Das Page 2
5/2/2019 19:17

03 Tanmoy Das Page 9
5/2/2019 19:17

04 Tanmoy Das Page 10
5/2/2019 19:17